9-2019

More Anatomically Realistic and Quantitative Models of Pulmonary Surfactant Action and Alveolar Stability

Charles F. Babbs
Purdue University, babbs@purdue.edu

More anatomically realistic and quantitative models of pulmonary surfactant action and alveolar stability

Charles F. Babbs, MD, PhD
Weldon School of Biomedical Engineering, Purdue University,
West Lafayette, Indiana, 47907, USA

September, 2019

ABSTRACT

To explore basic mechanisms of action of pulmonary surfactant in preventing alveolar collapse, a first-principles analysis is done analyzing forces on the shared walls separating adjacent alveolar gas bubbles. The analysis holds for concave alveolar models with either rounded, dome-like surfaces or flat, box-like surfaces. The analysis also holds for neighboring alveoli of varying size and shape. Surfactant action is characterized by two parameters describing reduction in surface tension vs. log concentration. The resulting equations describe the net pressure tending to shift the shared position of a wall, as a function of the perturbation from a balanced initial state. In the absence of surfactant, the bubbles exist in an unstable equilibrium. Any perturbation causes runaway positive feedback such that one bubble shrinks and the other enlarges. In the presence of surfactant having adequate concentration and potency the initial normal bubble volumes are maintained by stabilizing negative feedback. With borderline surfactant activity there is stable partial enlargement of one bubble and partial shrinkage of the other bubble. The present analysis shows quantitatively how pulmonary surfactant normally works to equalize the sizes of neighboring alveolar gas bubbles in small, local regions of lung. Once a threshold surfactant effect is exceeded this local stability is robust. However, inadequate surfactant can lead to microatelectasis, intrapulmonic shunting of venous blood past poorly alveoli, and arterial hypoxemia. The presence of giant alveoli surrounded by smaller collapsed alveoli, as well as the presence of hyaline membranes, characteristic of respiratory distress syndrome of the newborn, are also explained by the underlying biomechanics.

Keywords: alveolar collapse, alveoli, atelectasis, hyaline membrane disease, neonatal, RDS, respiratory distress syndrome of the newborn, surface tension.

1. INTRODUCION

Normal lung function depends upon the presence of a pulmonary surfactant, a complex mixture of detergent-like molecules that stabilizes the sizes of alveolar gas bubbles, presumably by reducing surface tension. Lack of sufficient surfactant at birth results in respiratory distress syndrome (RDS) of the newborn, a severe lung disease that can be reversed by treatment with intrapulmonary natural or semi-synthetic surfactants[1]. In patients experiencing prolonged cardiopulmonary bypass for cardiac surgery there can be patchy atelectasis associated with decreased pulmonary surfactant ("pump lung")[2]. There is also a decrease of surfactant in the lungs of cigarette smokers[3] and in cases acute respiratory distress syndrome (ARDS) with surfactant insufficiency.

Natural pulmonary surfactant is a mixture of dipalmitoylphosphatidylcholine (DPPC), other phospholipids, neutral lipids, hydrophilic and hydrophobic apoproteins (SP-A, B, C, and D), and other proteins[4, 5]. In healthy individuals, pulmonary surfactant is secreted by Type II alveolar cells and distributes to the surfaces of alveolar gas bubbles. The phospholipids have hydrophilic "heads" and hydrophobic "tails", and are thought to distribute on the surface of the alveolar gas bubble with their tails facing the bubble lumen, reducing surface tension as a function of their concentration per unit area. The surfactant layer can be oligolamellar, rather than a true monolayer layer[6]. Natural lung surfactant contains less than 40% of the most effective, disaturated phospholipids, such as DPPC. Accordingly, increased surfactant activity may happen by a "squeeze out" mechanism[5], in which less effective surfactants in the mixture, such as unsaturated phosphatidylcholine (PC) and phosphatidylglycerol (PG) are squeezed out of the surface monolayer, if its surface area decreases, increasing or enriching the concentration of DPPC, which has two hydrophobic alkyl chains[7] and can be over 100 times more effective than the corresponding monomeric phospholipids[8]. This squeeze out model predicts that as bubble size decreases, the effective DPPC concentration increases, and in turn, the surface tension decreases.

Classical studies[9] repeated many times[10-12] demonstrate that elastic recoil pressures in lungs inflated with saline solution are substantially less at any given volume than those measured in lungs inflated with air. This simple experiment demonstrates air-water surface tension is responsible for a large part of the elastic recoil pressure of the lungs. That is, the larger part of the total retraction forces of the lung is ascribable to forces of surface tension.

Early on, 20th century textbooks of physiology described the tendency of alveolar gas bubbles to collapse, and the corresponding physiological importance of surfactant in reducing surface tension, using the law of Laplace (tension = transmural pressure × radius / 2) applied to two spherical alveolar gas bubbles, connected by branched tubular airways—a "ball and stick" or "balloon and tube" model (Figure 1)[13].

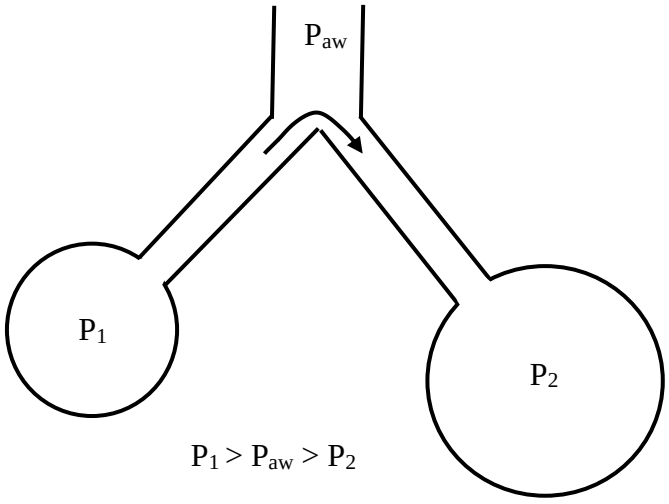

Figure 1. Traditional balloon and tube model explaining alveolar instability without surfactant. At certain critical times in the ventilatory cycle there can be net transfer of gas from smaller to larger alveoli in the absence of pulmonary surfactant.

An emergent property of this model and is that if a smaller Laplacian bubble of radius, r_1, is connected internally to a larger one of radius, r_2, with the same surface tension, T, then there is a tendency for unequal pressure, $P_1 = 2T/r_1 > P_2 = 2T/r_2$, to force air from the smaller bubble into the larger one, at least during certain brief intervals in the ventilation cycle when $P_1 > P_{aw} > P_2$ for common airway pressure, P_{aw} .

This hypothetical system exhibits an unstable equilibrium. If $r_1 = r_2$ exactly, the interconnected bubbles remain the same size. If one or the other radius is changed, however, the smaller one will collapse into the larger one, creating an abnormal state quite similar to that observed in respiratory distress syndrome (RDS) of the newborn, in which there is a deficiency of pulmonary surfactant and in which microscopically, a small number of hyperinflated alveoli are seen, surrounded by a larger number of collapsed alveoli[14].

In a general and qualitative way, it is suggested that pulmonary surfactant can stabilize this system by reducing surface tension, either in a crude sense by reducing surface tension to zero or to negligible levels, so that the Law of Laplace becomes irrelevant, or in a more sophisticated sense by reducing surface tension in an area-dependent manner, when a constant amount of surfactant is distributed over a varying alveolar surface area. As alveolar radius, r, decreases, the area becomes less and the surfactant concentration increases, which in turn reduces surface tension, opposing the tendency of the smaller gas bubble to collapse.

In addition to being qualitative, and not quantitative, this simple Laplacian model has been critically challenged by a number of thinkers. Prange[13] has suggested that "the Y-tube model of the alveolar inflation and the bunch-of-grapes model of alveolar anatomy deserve a place, not in

our minds and textbooks, but in the museum of wrong ideas". This critique is based upon several major differences between the assumed architecture of the model and the actual microscopic anatomy of the lung. In particular, (1) alveoli are not shaped like spheres; they are shaped like multifaced polyhedra, open on one side, with multiple flat sided facets. (2) Alveoli are not directly connected to the smallest tubular airways, but rather clustered together in alveolar ducts or sacs. They do not resemble individual balloons; rather, they have a sponge-like open architecture, arranged around the common atrium of the alveolar sac. (3) Alveoli often share common walls and are often directly interconnected by small alveolar pores of Kohn.

Fung[15] has also emphasized that at the alveolar level the balloon and tube model is "topologically wrong" and "both sides of each pulmonary alveolar septum are exposed to air at the same pressure". Further issues with the balloon and tube model have been raised by Hills[16], who suggested that "the validity of the conventional bubble model is clearly dependent on near-zero surface tension (< 5 mN/m)", as well as other shortcomings[17]. Nevertheless, this model continues to be taught in the 21st century, appearing in review articles[18], in textbooks[19-21] and in online study guides, lecture notes, flashcards, and You-Tube videos (For examples, search "Law of Laplace and alveolar collapse".)

The present paper presents a revised and neoclassical model of alveolar collapse and stability that preserves the simplicity and explanatory power of the original two bubble model but circumvents some of its anatomic limitations. This new model is also quantitative rather than qualitative. The essential feature is that neighboring alveoli within the same alveolar sac (or back-to-back neighboring sacs) have shared, common walls between them, such that the forces created by surface tension in neighboring bubbles oppose each other. In the absence of surfactant, any pair of side by side or back to back bubbles is unstable, because if one bubble gets slightly smaller, the opposing pressures on the shared wall will become unbalanced, shifting the wall further toward the smaller bubble. Thereafter, owing to the tendency of surface tension to minimize the surface area, the smaller bubble will assume a roughly similar, but smaller shape, and the larger bubble will assume a roughly similar but larger shape, subject to local boundary conditions. This cycle will be repeated in a runaway fashion, causing the arrangement of "giant alveoli", surrounded by many smaller, mostly collapsed alveoli, which are characteristic of respiratory distress syndrome of the newborn.

This simple system of adjacent bubbles is easy to analyze in terms of the underlying biophysics and may describe the essential features of alveolar collapse in conditions such as respiratory distress syndrome of the newborn. What follows is a quantitative description of the underlying biomechanics for either round sided or flat sided alveolar models. The dose-effect curve for surfactant and the critical amount of surfactant needed to stabilize the system are also specified quantitatively. The bubble equations and the surfactant equations are combined to create a mathematical model of alveolar stability.

2. THEORY

2.1 More atomically realistic model

As an alternative to the traditional balloon and tube model, Figure 2 illustrates a more anatomically realistic, neoclassical model, which includes adjacent alveolar gas bubbles in a particular alveolar duct or sac. These bubbles share walls with other alveoli, either in the same alveolar sac (bottom) or in a neighboring alveolar sac (top). The alveolar gas bubbles are of an arbitrary, concave, or dome-like shape, resembling partial pohyhedra, having a characteristic length, s, such as the time-averaged diameter over one ventilatory cycle. (The change in volume over a ventilatory cycle of normal quiet breathing is only about 7%[**].) The neighboring alveolar gas bubbles tend to make contact by way of the shared flat surfaces of the polyhedra (shaded region in Figure 2).

Now consider a movable patch of the shared wall between bubbles 1 and 2 having an arbitrary shape and constant area, a_{wall}. Let this patch be denoted W. Note that W may or may not contain a small alveolar pore. Consider also the partial perimeters, shown as dotted curves in Figure 2. These perimeters are selected such that the force of surface tension along each perimeter is perpendicular to W.

[**] To estimate the change in diameter during normal quiet breathing, where volume, V, is proportional to the cube of side length, s, we can use $\frac{V-\Delta V}{V} = 1 - \frac{\Delta V}{V} = \left(1 - \frac{\Delta s}{s}\right)^3$ or $\frac{\Delta s}{s} = 1 - \sqrt[3]{1 - \frac{\Delta V}{V}}$. For example, in an adult, we might have V = FRC + TV = 2500 ml and ΔV = TV = 500 ml, with ΔV/V = 1/5 and Δs/s ≈ 0.07. Similarly, in a neonate we might have V = FRC + TV = 35 ml/kg and ΔV = TV = 7 ml/kg, with ΔV/V = 1/5 and Δs/s ≈ 0.07.

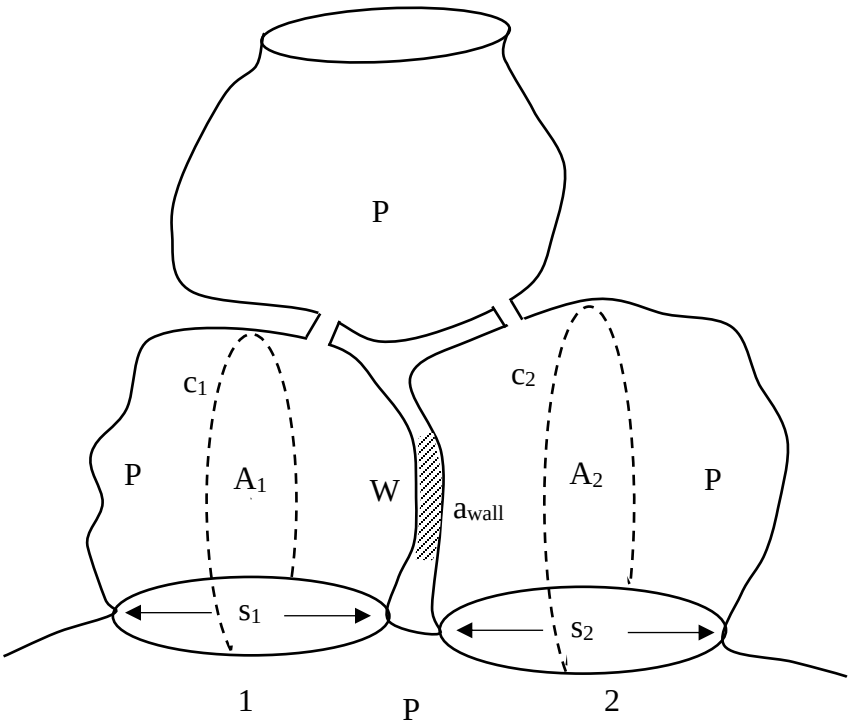

Figure 2. Sketch of alternative biomechanical model of three adjacent alveolar gas bubbles sharing common walls, some of which might include alveolar pores. Target patch, W, of shared wall having area, a_{wall}, is shown as shaded region. Airway pressure, P, is locally uniform. The gas bubbles may have arbitrary, dome-like shapes, ranging from partial spheres to flat sided boxes. Characteristic dimensions s_1 and s_2 may differ. The walls may be smooth or may be buckled or wrinkled in partial collapse.

Let the partial circumference of this perimeter in a plane parallel to wall W in bubble 1 be denoted c_1 , and let the area of the plane of the perimeter parallel to the surface of W be denoted A_1 . Let the partial circumference of the corresponding perimeter in bubble 2 be denoted c_2 , and let the corresponding plane area be denoted A_2 . For bubbles of characteristic lengths, s, the circumferences, c, are proportional to s, and the areas A are proportional to s^2, so that

$$\frac{c}{A} = \varphi \frac{1}{s} \qquad (1)$$

for a shape factor, φ . For hemispheres of diameter, d = s, open at the bottom, the shape factor is $\frac{c}{A} = \varphi \frac{1}{s} = \frac{\frac{1}{2}\pi d}{\frac{1}{2}\pi\left(\frac{d}{2}\right)^2}$, so that φ = 4. Similarly, for a half hexagon, open at the bottom, the

corresponding shape factor is 4.62, and for a full hexagon, open at the bottom at one side, the shape factor is 3.85 (calculations not shown). Most compact alveolar geometries would have shape factors near 4.[**] Hence, *in vivo*, shape factors may differ modestly, but not greatly.

If wall patch, W, moves from left to right in Figure 2, then the volume of bubble 1 will expand and the volume of bubble 2 will shrink. Because the walls of each bubble have surface tension, they will adjust to form minimal surface area shapes of the same general design, such as hemispheres or boxes, depending on the local anatomical constraints provided by the tensile matrix of connective tissue in the alveolar septae. However, the movement of the shared wall still allows one bubble to expand and the other bubble to contract.

Now consider the balance of forces acting on W, with forces acting on area, a_{wall}, from left to right in Figure 2 considered positive. In bubble 1 the force from internal pressure, P, on the shared wall is Pa_{wall} . This force is opposed by surface tension, T_1, in bubble 1, which creates an inward directed force acting along the perimeter of the bubble in a direction normal W. This counterbalancing horizontal force from wall tension opposes the force of gas pressure on W. The magnitude of the net force from bubble 1 pushing on W from left to right is

$$F_1 = Pa_{wall} - T_1 c_1 \frac{a_{\text{wall}}}{A_1} \ . \qquad (2)$$

Here the total force of surface tension is T_1c_1. The fraction $\frac{a_{wall}}{A_1}$ describes the proportion of the total force of surface tension acing on W. Similarly, the magnitude of the net force from bubble 2 pushing on W from right to left is

$$F_2 = Pa_{wall} - T_2 c_2 \frac{a_{wall}}{A_2} \ . \qquad (3)$$

Because the two alveoli are derived from the same alveolar sac or very closely neighboring alveolar sacs, as well as because of the presence of alveolar pores, the air pressure, P, has the same magnitude in both alveoli. The net pressure difference across W in the positive, left to right (1 to 2) direction is

$$P_{net} = \frac{F_1 - F_2}{a_{wall}} = T_2 \frac{c_2}{A_2} - T_1 \frac{c_1}{A_1} = \frac{T_2 \varphi_2}{s_2} - \frac{T_1 \varphi_1}{s_1} , \qquad (4)$$

for shape factor, φ, which may change as a function of s_1 and s_2. (A similar analysis for one sided, but not counterbalancing, retraction forces at plane interfaces was described in the year 1975 by Reifenrath[22] (pages 123-124)). Now, without surfactant, if $T_1 = T_2 = T$, the common

[**] For cubes of side, s, open at the bottom, for example, the shape factor is $\frac{c}{A} = \varphi \frac{1}{s} = \frac{3s}{s^2}$, so that φ = 3. For tall, narrow open-bottom rectangles of short side, s, and tall side, b, the shape factor, φ = (2b+s)/(bs), approaches 2 as short side span, s, approaches zero. For short, wide open-bottom rectangles of wide side, s, and short side, b, the shape factor, φ = (2b+s)/(bs), approaches infinity as b approaches zero. If one bubble collapses into its neighbor there might be some systematic change in the shape factor, opposed to some degree by the effects of surface tension that minimize surface area and perimeters toward more compact configurations.

surface tension of water, and if $\varphi_1 = \varphi_2$ for simplicity, then equation (4) clearly implies positive feedback. As the wall moves from left to right, bubble 1 will get bigger and bubble 2 will get smaller, further increasing the net positive pressure on W.

To characterize the size relative changes of neighboring alveolar gas bubbles, let ε denote the absolute value of the fractional change in bubble dimensions, $\frac{|\Delta s|}{s}$, caused by movement of W, where s is the average initial value of local alveolar dimensions during the ventilatory cycle, and $|\Delta s|$ is the absolute value of septal shift in Figure 2. In this case surfactant concentration in each bubble wall changes as a function of $\varepsilon_1 = \frac{|\Delta s|}{s_{10}}$ and of $\varepsilon_2 = \frac{|\Delta s|}{s_{20}}$ with subscript 0 indicating the initial conditions. Then $s_1 = s_{10}(1 + \varepsilon_1)$ and $s_2 = s_{20}(1 - \varepsilon_2)$.

2.2 Surfactant effect

A remarkable property of the surfactant that coats the walls of alveolar gas bubbles is that it reduces the surface tension by a factor of up to fifteen[23-25]. Surfactants typically reduce surface tension in a concentration-dependent manner, as shown in Figure 3. The semi-logarithmic relationship is that most frequently found experimentally[8, 26, 27]. Surface tension of saline at 37°C , T_{max}, is about 70 mN/m[7]. For tiny concentrations of surfactant, there is no effect. Then after a critical minimal concentration, c_0 , is reached, the "breaking point" of the curve, surface tension decreases as a linear function of the logarithm of the concentration until a maximal reduction is achieved, after which further increases in surfactant concentration have no additional effect. As shown in Figure 3, curves of this type can be described simply by the piecewise linear function of the log surfactant concentration, c , in the liquid phase as follows:

$T = T_{max}$, $c < c_0$

$$T = T_{max}\left(1 - \beta \frac{ln(c/c_0)}{ln(c_{max)}/c_0)}\right), \quad c_0 \le c \le c_{max} \qquad (5)$$

$T = T_{max}\,(1 - \beta)$, $c > c_{max}$,

where β is the maximal fractional reduction in surface tension produced by a particular surfactant, which is a measure of its "pharmacodynamic effect".

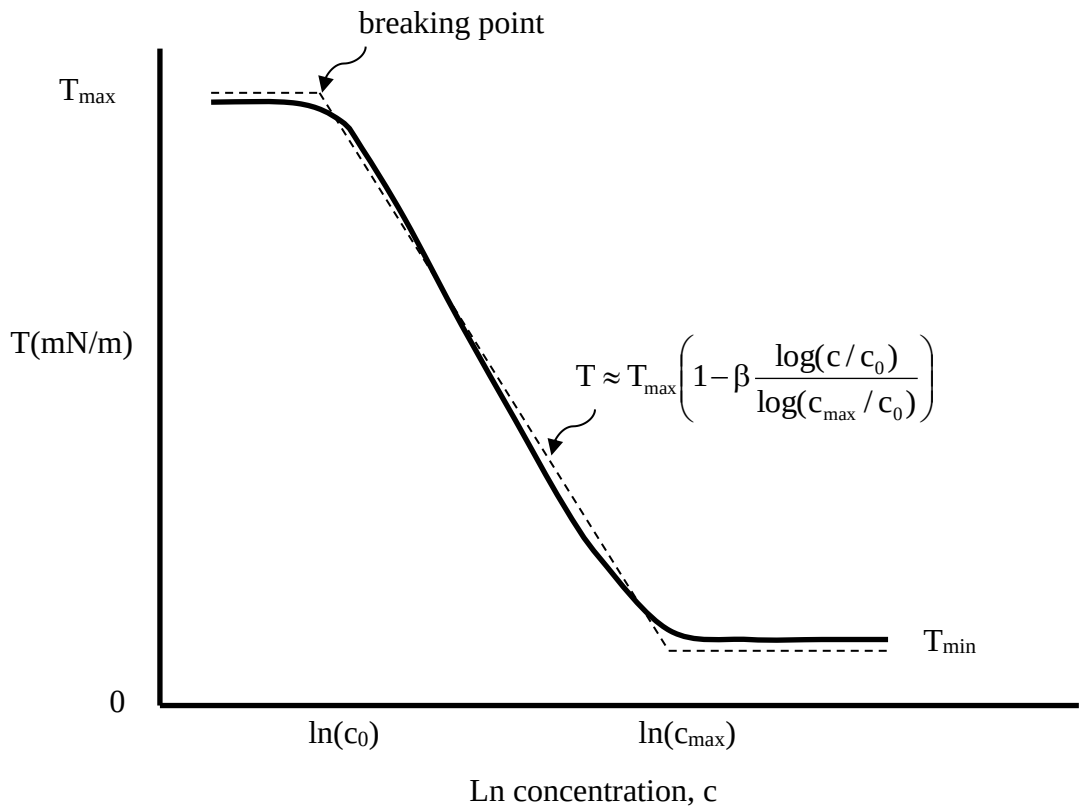

Figure 3. Typical dose response curve for a surfactant redrawn from (Trillo, 2014)[8]. Dashed curve shows piecewise linear approximation. Ln indicates the natural logarithm.

Initially, the time-averaged concentration of surfactant on the surface of each alveolar bubble is some specified nominal or normal value, c_n , which we assume in the present model is constant over the many cycles of ventilation, such that for variable concentration, c(ε), we have $cs^2 = c_n s_n^2$ or $cs_n^2(1+\varepsilon)^2 = c_n s_n^2$. , where, as before, the variable, ε, denotes the fractional change in gas bubble size. The influence of relative area on local surfactant concentration during small changes in alveolar volume has been demonstrated experimentally[28-30] and theoretically[31]. In this case the concentration as a function of ε is $c = \frac{c_n}{(1+\varepsilon)^2}$, and in the critical range of interest to the right of the breaking point, $c_0 \le c \le c_{max}$,

$$T = \mathrm{T}_{max}\left(1 - \beta\frac{ln\left(\frac{c_n}{c_0}\frac{1}{(1+\varepsilon)^2}\right)}{ln\left(\frac{c_{max}}{c_0}\right)}\right), \tag{6}$$

or

$$T = \mathrm{T}_{max}\left(1 - \beta\frac{ln\left(\frac{c_n}{c_0}\right) - 2ln(1+\varepsilon)}{ln\left(\frac{c_{max}}{c_0}\right)}\right). \tag{7}$$

Introducing the dimensionless constants

$$a = 1 - \beta\frac{ln\left(\frac{c_n}{c_0}\right)}{ln\left(\frac{c_{max}}{c_0}\right)}, \tag{8}$$

and

$$b = \beta\frac{2}{ln\left(\frac{c_{max}}{c_0}\right)}, \tag{9}$$

to describe the nominal concentration and potency of a particular surfactant, then

$$T = T_{max}(a + b\,ln(1+\varepsilon)). \tag{10}$$

Constant, a , represents the fractional reduction in T before any wall shift, when ε = 0. That is, $a = T/T_{max}$. Moreover, accounting for surfactant effect, when the bubble dimension increases by ε , surface tension increases, rather than remaining constant, as shown experimentally by Smith and Stamenovic[32].

2.3 Combined force balance and surfactant effects

Now, as before, let ε denote the absolute value of the fractional change in bubble dimensions, $\frac{\Delta s}{s}$ that is caused by movement of W, where s is the average initial value of local alveolar dimensions in time during the ventilatory cycle. In particular, $s_1 = s_{10}(1 + \varepsilon_1)$ and $s_2 = s_{20}(1 - \varepsilon_2)$. Then the pressure difference across the shared wall between neighboring bubbles is simply

$$P_{net} = \frac{T_2\varphi_2}{s_{20}(1-\varepsilon_2)} - \frac{T_1\varphi_1}{s_{10}(1+\varepsilon_1)} . \quad (11a)$$

To add the effect of a modest change in shape factor, φ, which in view of the forgoing examples will be most likely within the range of about 3.5 to 4.5, as neighboring bubbles stretch and shrink; consider a simple linear model. In this sub-model dφ/ds = k, a small constant. Then $\varphi_1 = \varphi_{10}(1 + k\varepsilon_1)$ and $\varphi_2 = \varphi_{20}(1 - k\varepsilon_2)$. That is, as wall shift occurs, bubble 1 may become a little more rounded with φ closer to 4, and bubble 2 may become a little more flattened with φ closer to 3. For this varying shape factor model

$$P_{net} = \frac{T_2\varphi_{20}(1-k\varepsilon_2)}{s_{20}(1-\varepsilon_2)} - \frac{T_1\varphi_{10}(1+k\varepsilon_1)}{s_{10}(1+\varepsilon_1)} . \quad (11b)$$

For neighboring bubbles differing in initial size but remaining similar in shape k = 0. The goal in what follows is to explore the stability of the neighboring bubble system in response to small mechanical changes, ε, in the alveolar dimensions caused, for example, by slight differences in lung elastic recoil, or perhaps small transient differences in patency of respiratory bronchioles serving neighboring alveolar sacs.

Substituting surfactant dependent surface tensions for T_1 and T_2 in Equation (11b),

$$P_{net} = T_{max}\left(\frac{(a+b\,ln(1-\varepsilon_2))\varphi_{20}(1-k\varepsilon_2)}{s_{20}(1-\varepsilon_2)} - \frac{(a+b\,ln(1+\varepsilon_1))\varphi_{10}(1+k\varepsilon_1)}{s_{10}(1+\varepsilon_1)}\right) . \quad (12)$$

For purposes of perturbation analysis for any particular pair of alveoli, consider an initial equilibrium, which may or may not be stable, as the starting point for the analysis. In this starting scenario we would have $\varepsilon_1 = \varepsilon_2 = 0$, and also $P_{net} = 0$. Then $0 = \left(\frac{\varphi_{20}}{s_{20}} - \frac{\varphi_{10}}{s_{10}}\right)$, or $\frac{\varphi_{20}}{s_{20}} = \frac{\varphi_{10}}{s_{10}} \equiv K$, a constant. Now for purposes of perturbation analysis for any particular pair of alveoli, we can consider dimensionless pressure difference across a particular patch of shared alveolar wall, $P_{net}/(KT_{max})$, as

$$p = \frac{(a+b\,ln(1-\varepsilon_2))(1-k\varepsilon_2)}{1-\varepsilon_2} - \frac{(a+b\,ln(1+\varepsilon_1))(1+k\varepsilon_1)}{1+\varepsilon_1} . \quad (13a)$$

Further, because of the wall shift with dimension s_1 increasing and dimension s_2 decreasing, each by the same absolute amount, $\Delta s = \varepsilon_1 s_{10} = \varepsilon_2 s_{20}$, we have $\varepsilon_2 = \frac{s_{10}}{s_{20}}\varepsilon_1 \equiv \lambda\varepsilon_1$ for constant λ depending on the initial size difference in alveolar gas bubbles 1 and 2. In this case

$$p = \frac{(a+b\,ln(1-\lambda\varepsilon_1))(1-k\lambda\varepsilon_1)}{1-\lambda\varepsilon_1} - \frac{(a+b\,ln(1+\varepsilon_1))(1+k\varepsilon_1)}{1+\varepsilon_1} \tag{13b}$$

for $-1 < \varepsilon_1 < \lambda\varepsilon_1$, as a function of ε_1 only.

When the fractional change in bubble size, $\varepsilon_1 = 0$, then $p = 0$, as expected.

In this way the neighboring bubble model and the surfactant effect model can be combined to describe the critical equilibriums for airway collapse or stability in terms of runaway or compensatory motion of the shared wall. All model parameters are defined on the basis of physics, anatomy, chemistry, and physiology. There are no free parameters or arbitrary constants.

2.4 Values of critical constants

Analysis of experimental data can be done to find the values of constants a and b in Equation (13b). For normal alveoli the surfactant concentration c_n produces an in vivo surface tension of 25 mN/m[23] in vitro in experiments on surfactant bubble films, and values ranging from about 10 to 25 mN/m in vivo[33, 34]. Taking a value of 18 mN/m as the initial operating point for our model, and taking 70 mN/m as the surface tension for saline solution without surfactant, the value for constant, a, in Equation (11) becomes

$$a = \frac{T}{T_{max}} = \frac{18}{70} \approx 0.257. \tag{14}$$

All that is needed to estimate constant, b, are two measured points in the linear range of surface tension vs. log concentration, as described in the Appendix. Point 1 represents a state of high surface tension and low surfactant concentration, and point 2 represents a state of lower surface tension and increased surfactant concentration. As explained in the Appendix, the critical variables for data analysis are $\ln(c_2/c_1)$ and $(T_1 - T_2)/T_{max}$, where T_{max} is the surface tension of saline solution without surfactant.

The specific data dependent value for constant, b, in Equations (10) through (13b) is given by

$$b = 2\frac{(T_1-T_2)/T_{max}}{ln(c_2/c_1)} \tag{15}$$

with T_{max} = 70 mN/m for saline solution, and the other variables coming from two measured data points in a particular experiment, as shown in Table 1. A virtue of this approach is that only relative values are needed, so concentration ratios can be inferred from measured bubble area ratios, if necessary.

Table 1 presents the results of this analysis to extract representative values of constants a and b from nine published experimental studies involving natural and synthetic surfactants. There is a range of effectiveness of the surfactants in terms of lumped parameter, b. A middle value for use in the standard model is b = 1.34, the average observed value.

TABLE 1. *Curve fit constants from experimental data.* $\Delta T = T_1 - T_2$.

Investigator (year)	$2\Delta T/T_{max}$	$\ln(c_2/c_1)$	**b**
Hallman (1976)	1.229	1.609	0.763
Barrow (1979) Fig 1	0.514	0.470	1.094
Schurch (1989) Fig 5	0.529	0.693	0.763
Seeger (1999) mixture	0.714	1.609	0.444
Seeger (1999) Curosurf	0.457	0.511	0.895
Walters (2000)	0.857	0.490	1.751
Possmayer (2001)	0.714	0.211	3.390
Scurch (2001)	0.714	0.375	1.906
Trillo (2014) Fig 5	0.714	0.693	1.030
Average			1.337

To estimate the size difference factor, λ, consider that most neighboring alveoli in a cluster will be of similar size initially, with size difference factor, λ, being somewhat greater than 1.0 in some cases and somewhat less than 1.0 in other cases. For an average or "typical" alveolus one would expect $1+ \lambda \approx 2$.

To estimate shape-change factor, k, we can expect on the basis of the forgoing geometric analysis and the various test shapes that a typical normal alveolar shape constant would be $\varphi \approx 4$. This is the most likely scenario. In cases where there is systematic change in shape factor with septal shift, the range of φ would be perhaps 3.5 to 4.5. Thus for $\varepsilon = 1$ we would have $4.5/4 = 1 \pm k$, depending on which way the shape factor changes under local conditions. Hence, we might expect $k \approx \pm 0.125$. An approximate working value for a standard model would be $k = 0$. To explore possible reasonable changes in shape factor, one can study $-0.2 \leq k \leq 0.2$.

3. RESULTS

3.1 Linear approximations

Before proceeding to exact numerical calculations, it is insightful to solve Equation (13b) analytically for some simplified test cases. For small perturbations such as $\varepsilon_1 = \Delta s/s_1 << 1$, both the inverse function and the logarithmic function of can be simplified using binomial series or Taylor series expansions,

$$\frac{1}{1+\varepsilon} \approx 1 - \varepsilon + \varepsilon^2 - \varepsilon^3 + \cdots \tag{16}$$

and

$$ln(1+\varepsilon) \approx \varepsilon - \frac{1}{2}\varepsilon^2 + \frac{1}{3}\varepsilon^3 + \cdots. \tag{17}$$

Dropping terms for powers of $\varepsilon > 1$ for small perturbations, the mathematics of Equation (13b) become more clear. After using Equations (16) and (17) in Equation (13b), the dimensionless transmural pressure difference, as a function of the fractional expansion, ε_1, of bubble 1 is

$$p(\varepsilon_1) \approx (1+\lambda)(a(1-k)-b)\varepsilon_1, \tag{18}$$

and the slope of the dimensionless transmural pressure,

$$\frac{dp}{d\varepsilon_1} \approx (1+\lambda)(a(1-k)-b). \tag{19}$$

In the case of zero surfactant concentration the constant, a = 1, and the slope, β, in Figure 3 is zero, so that b = 0. The transmural pressure is proportional to any small volume offsets. Equations (18) and (19) imply positive feedback and runaway collapse over the full range $-1 \le \varepsilon \le 1$. However, for a particular surfactant compound, characterized by b > 0 , the value of $a = 1 - \beta \frac{ln\left(\frac{c_n}{c_0}\right)}{ln\left(\frac{c_{max}}{c_0}\right)}$ becomes smaller, as the surfactant concentration, c_n, becomes greater. Eventually, for a(1 – k) < b , the slope of Equation (18) becomes less than zero over the full range $-1 \le \varepsilon_1 \le 1$. Now if gas is shifted from bubble 1 to bubble 2 by some initial perturbation, the wall of bubble 2 will be pushed backward into bubble 1, restoring equilibrium. Moreover, the greater the initial offset, ε_1, in the positive direction, the more the compensating negative pressure difference. Similarly, for a negative offset, $\varepsilon_1 < 0$, Equation (18) implies that for a(1 – k) < b there will be compensating pressure in the positive direction. Under these conditions the system is stable.

3.2 Shared wall pressure

Figure 4 shows the exact solutions without surfactant (a = 1, b = 0) for shared wall pressure (Equation (13)) compared with the linear approximation (Equation (18)) as a function of the perturbation volume fraction, ε_1, for the two-bubble model. The point at $\varepsilon_1 = 0$ is the neutral or equilibrium position. In the absence of surfactant, however, the origin is an unstable equilibrium. The same type of positive feedback and runaway collapse is predicted by both the exact and approximate solutions.

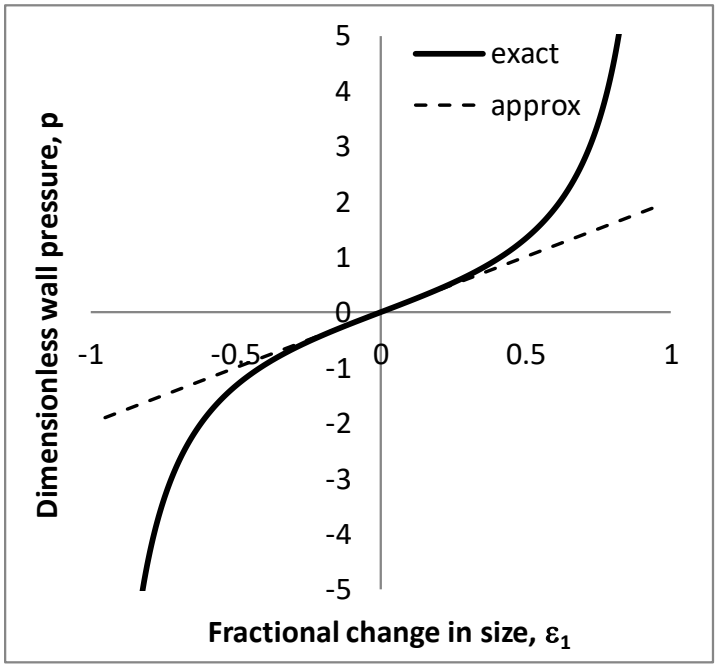

Figure 4. Perturbation analysis using transmural pressure without surfactant (a = 1, b = 0) as a function of the fractional offset, ε_1, in linear dimension. Curves represent exact and approximate solutions. For shape factor 4, one dimensionless unit on the vertical axis equals $\frac{4 \cdot 0.070\ N/m}{0.0001\ m} \cdot \frac{0.0075\ mmHg}{N/m^2} = 21\ mmHg$ *. Shape parameters* λ *= 1 and k = 0.*

Figure 5 shows the exact solutions with a mid-range concentration of a surfactant with properties similar to that of biological pulmonary surfactant (Table 1). The chart shows dimensionless transmural pressure, p, (Equation (13b)) and the linear approximation (Equation (18)) as a function of the fractional perturbation in alveolar size, ε_1 , for the side by side, two-bubble system. Now, for either the exact or approximate solutions, when the perturbation is positive, the resulting wall pressure difference is negative, stabilizing the volumes of both bubbles. A stable zero crossing point occurs at $\varepsilon_1 = 0$, since the slope of the function is negative at the zero crossing. The magnitude of the compensating pressure is physiologically meaningful, on the order of 20 mmHg per unit of dimensionless pressure.

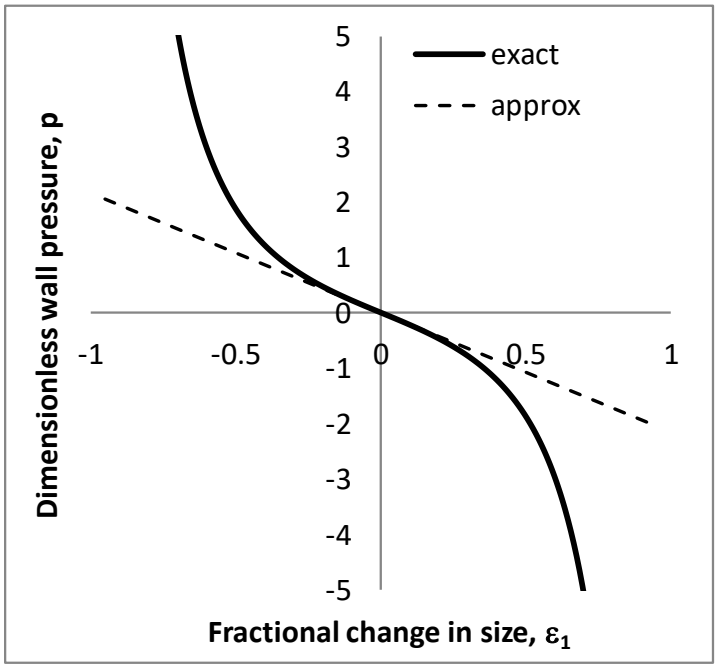

Figure 5. Perturbation analysis with surfactant. a = 0.257, b = 1.34 , k = 0.0, λ = 1 (standard normal model). A normal concentration and potency of surfactant can stabilize the system for all possible perturbations. Curves represent exact and approximate solutions. For shape factor 4, one dimensionless unit on the vertical equals $\frac{4 \cdot 0.070\ N/m}{0.0001\ m} \cdot \frac{0.0075\ mmHg}{N/m^2} = 21\ mmHg$.

If an effective surfactant is present in sufficient concentrations, the origin is a stable equilibrium (Figure 5). In general, if the wall pressure function, $p(\varepsilon_1)$, is constrained to the "unstable quadrants" 1 and 3 in Cartesian coordinates, there will be an unstable equilibrium. If the function $p(\varepsilon_1)$ is constrained to the "stable quadrants" 2 and 4 in Cartesian coordinates, there will be a stable equilibrium. For the particular values of constants a and b in Figure 5 there is stability over the complete dynamic range of ε_1 from –1 to 1. The results of Figure 5, which mimic the action of normal pulmonary surfactant, demonstrate the robustness of the surfactant effects over the entire range of possible wall shifts.

The physics of the two-bubble system with adequate surfactant effect ($a(1 - k) < b$), is analogous to the physics of a pendulum in the gravitational field at the Earth's surface or of a simple spring and mass system. If the mass at the end of the pendulum or at the end of the spring is pulled in one direction, there will be a proportional restoring force directed toward the equilibrium position. If the mass is pulled in the opposite direction there will be an oppositely signed restoring force directed toward the equilibrium position.

It is interesting to explore the region of transition between unstable and stable states for gradually increasing amounts of surfactant activity. Figure 6 illustrates the effects of a series of surfactant concentrations, specified by decreasing values of parameter, a . As surfactant action is increased, the slope of the shared wall pressure function gradually decreases from positive to negative. The greater the relative dose of the surfactant, the greater are the restoring pressures.

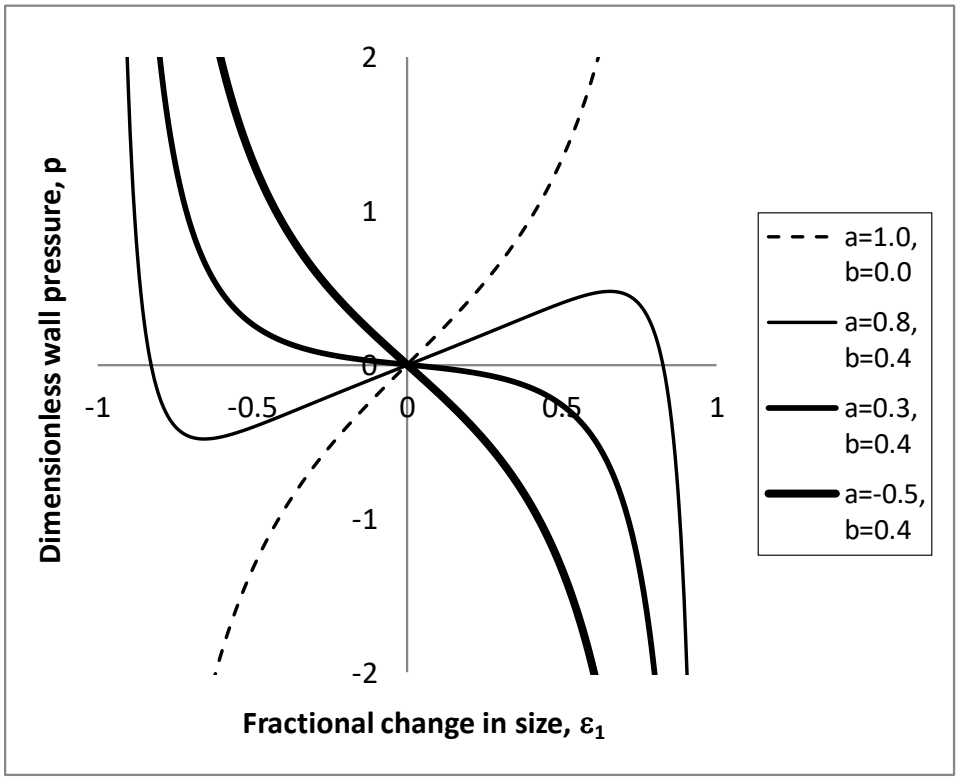

Figure 6. Perturbation analysis for increasing surfactant activity in terms of shared wall pressure. Decreasing values of parameter, a, including a < 0, correspond to increasing surfactant concentration. Shape parameters $\lambda = 1$ and $k = 0$.

A closer look at the transition region for the exact solutions reveals interesting behavior. For example, when a = 0.57 and b = 0.43 in Equation (13b) the results in Figure 7 are obtained. There is one unstable equilibrium, and there are two stable equilibriums. If a small positive wall shift, $\varepsilon_1 > 0$, occurs, then bubble 1 will continue to expand and bubble 2 will continue to shrink until the downward sloping zero crossing point in Figure 7 is reached. There the system becomes stable, because further positive wall displacement results in negative feedback. A similar phenomenon happens for a small negative offset, $\varepsilon_1 < 0$.

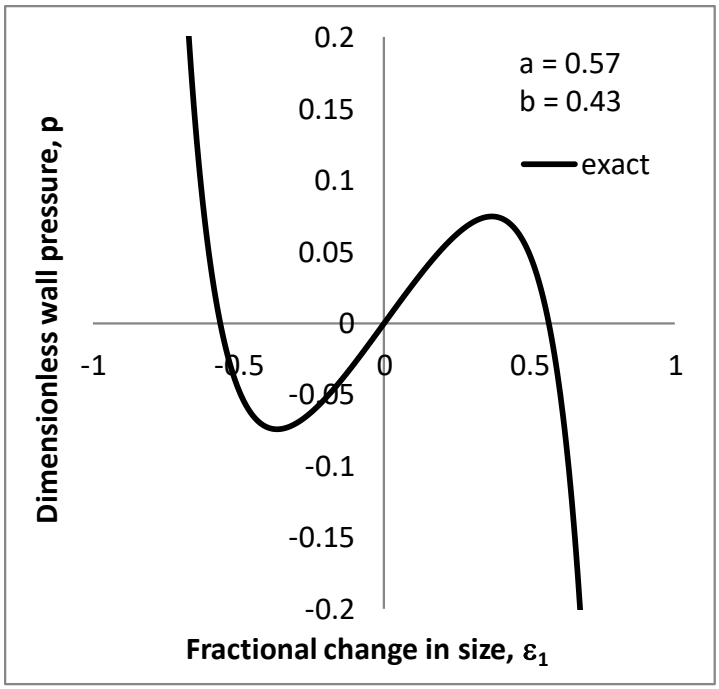

Figure 7. Perturbation analysis for a borderline case (a = 0.57, b = 0.43, λ = 1, k = 0). There are stable points at the two negatively sloping zero crossings near ±0.5. Note the expanded vertical scale compared to Figure 6.

3.3 Size and shape effects

Sensitivity of the results in Figures 4 through 7 to changes in the initial size mismatch factor, λ, and the shape factor change term, k, can be appreciated both analytically, by inspection of Equations (18) and (19), and also numerically by evaluation of Equation (13b) for test cases. Analytically, the slope of the stability function at $\varepsilon_1 = 0$ is given by Equation (19) as $dp/d\varepsilon_1 = (1+\lambda)(a(1-k)-b)$. The initial size mismatch factor, $\lambda = s_{01}/s_{02}$, is always greater than zero. Hence changes in λ will influence the magnitude of the slope somewhat, but not the sign of the slope. That is, to first order, changes in λ will not change the threshold between stability and instability of the two-bubble system. The system is essentially stable if $a(1-k) < b$, and unstable otherwise. Thus, changes in the absolute value of k, representing shape-factor change with gas transfer from one bubble to the other, will cause modest changes in the threshold conditions for stability. Values of $k < 0$ will make the system somewhat less stable, requiring greater surfactant activity to enforce stability. Values of $k > 0$ will make the system somewhat more stable, requiring less surfactant activity to enforce stability. The general requirement for some critical level of surfactant activity remains the same.

Figure 8 shows examples of numerical solutions for the exact expression of Equation (13b), including nonlinear as well as linear effects. In this highly sensitive, borderline stable case any changes in initial size mismatch parameter, λ, from the standard value of 1.0 cause subtle

changes in slope both in the linear and nonlinear portions of the curve. The same is true when the shape factor change term, k, is increased from 0 to 0.2 or decreased from 0 to – 0.2. Qualitative behavior of the two-bubble system with two stable equilibrium points at negatively sloping zero crossings is similar to that of the standard model in Figure 7.

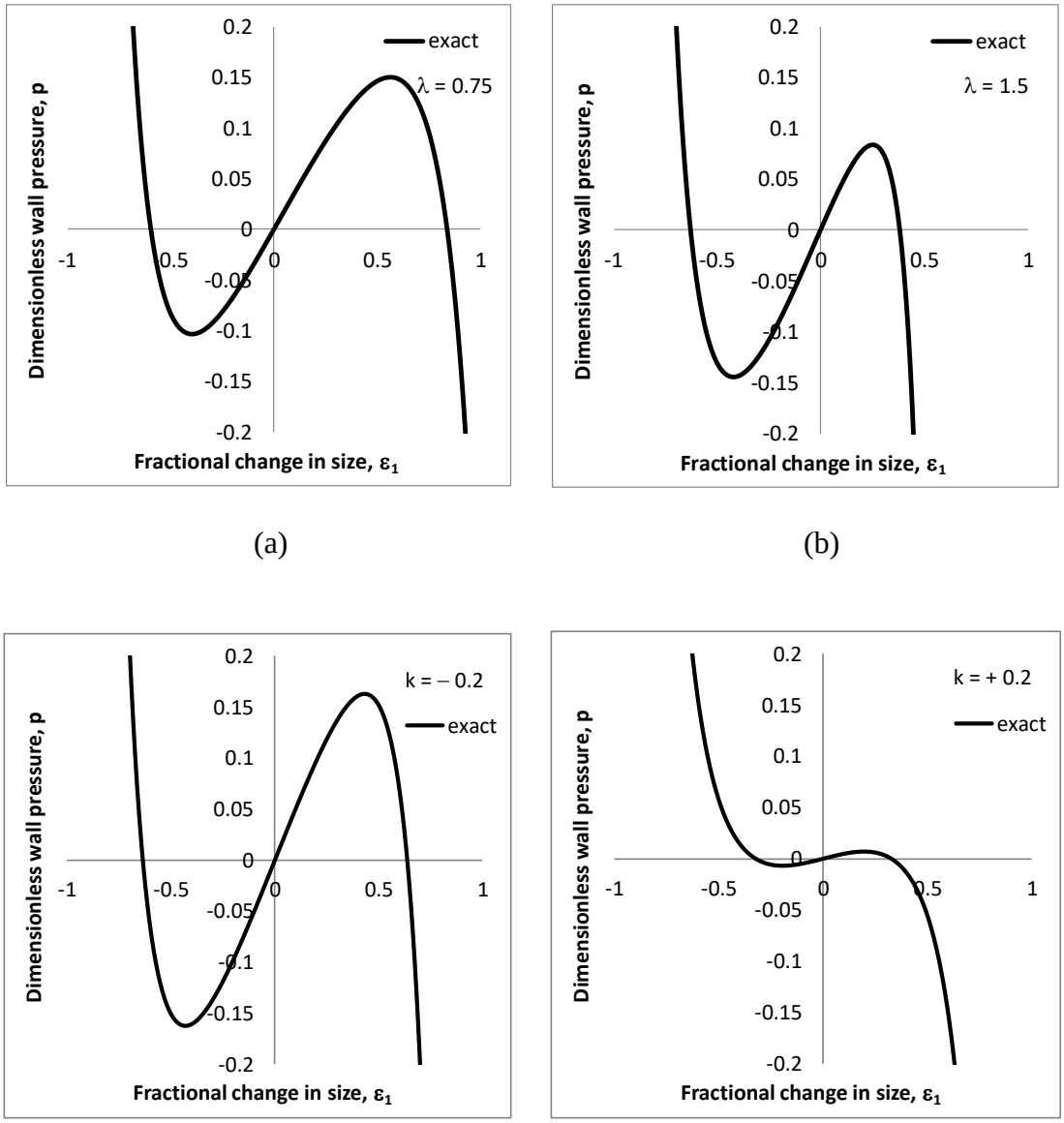

Figure 8. Sensitivity analysis for size and shape difference factors λ and k with a = 0.57, b = 0.43. When initial size mismatch parameter, λ, or shape factor change parameter, k, is changed, there are still stable points at the two negatively sloping zero crossings. Note the expanded vertical scales compared to Figure 6.

4. DISCUSSION

The conventional qualitative explanation for the role of surfactant is that, once interconnected, smaller bubbles would have higher internal pressures, and hence gas would flow from smaller bubbles into larger ones until the smaller bubbles collapsed. In this way it has been taught that surfactant protects against the collapse of alveoli and consequent formation of pulmonary edema, which would happen otherwise as the net collapse pressure draws fluid from capillaries into the alveolar spaces having smaller bubbles[3, 35], leading to the shunting of venous blood past unventilated alveoli, and profound arterial hypoxemia. In addition, the general reduction of surface tension by surfactant reduces lung recoil, ‘‘making breathing easy’’[36].

These teachings, however, are based on unrealistic anatomical assumptions that alveoli are spherical bubbles, connected only by tubular airways, rather than dome-like or box-like structures, often with flat sides, connected directly to the same alveolar sac and sharing common alveolar walls with their neighbors. Moreover, the original balloon-and-tube model, based on the Law of Laplace for spherical bubbles, is only qualitative or at best semi-quantitative. To fully understand the physiological mechanism that normally controls alveolar gas bubble size, and how it breaks down in conditions such as RDS, one needs to have a more anatomically realistic, quantitative model.

The balance of forces described by Equations (13a) and (13b) provides a compact, quantitative mechanism for the local instability of alveolar neighboring gas bubble size in the absence of adequate surfactant, as well as for the local stability of neighboring alveolar gas bubble size in the presence of adequate surfactant. The proposed mechanism for size stability works despite the many natural complexities of the underlying living system, which include the angled corners of non-spherical alveolar walls, deviation of the bubbles from a spherical shape at low surface tensions[37], the action of surfactant activity-boosting apoproteins[4], lipids[23], or drugs[38], possible degradation of surfactants by proteases or inhibition by plasma proteins[24], and the existence of surface tension–area hysteresis loops[3]. Moreover, the present approach easily incorporates possible molecular mechanisms other than simple monolayering for surface tension reduction. Such adjunct mechanisms include selective DPPC adsorption as well as recruitment of apoproteins during bubble compression from multilayered raft-like or iceberg-like reservoirs associated with the bubble surface[7, 37]. The same goes for synthetic or semi-synthetic surfactant preparations, including additives to enhance their activity[4]. Effects of such complexities can be incorporated into the lumped shape factor, φ, and the constants a and b.

An advantage of the present analysis and the associated mathematical model is that they accommodate neighboring alveoli of various sizes and shapes in the initial conditions. Data exist showing that the ratio of alveolar depth to alveolar mouth diameter changes with inflation under certain conditions. Klingele and Staub[39] measured the ratio of maximum depth to the opening or mouth diameter of alveoli in anesthetized cates. This ratio was constant (0.89 ± 0.02) for inflation volumes at and above 50% of maximum lobe volume. However, the ratio progressively increased for inflation volumes below 50%, indicating that the alveoli can became relatively narrower. Such narrowing would tend to produce larger shape factors, φ, in the present

mathematical model. There is one report that the alveolar septae may fold during deflation and unfold on inflation[40]; however the authors conclude that the "folds form *de novo* during experimental preparation; one need not postulate that septal folding was present in vivo." In addition, the ability of the present model to deal with initial conditions including different sized alveoli is useful in view of anatomic observations showing some differences in diameters of neighboring alveoli, even if the plane of section is taken into account[41].

It is important to appreciate that the present analysis and mathematical model describe neighboring alveoli in one alveolar sac. There is nothing in the mathematics that requires average local alveolar diameters to be the same in different lobes of the lung. The initial conditions are entirely local. The initial diameters, s_{10} and s_{20}, become part of the normalization factor for the scaled pressured difference, p, plotted in Figures 4 through 8. In such cases there could well be different normal equilibrium sizes, s_{01} and s_{02}, in different parts of the lung. However, local consistency in gas bubble size will still be maintained. Similarly, the present revised and augmented bubble model applies equally well to small animals with smaller alveolar diameters[43, 44] as well as to larger animals, such as humans, with larger alveolar diameters. Also, the diameters s_{10} and s_{20} can be regarded as time averaged values throughout a ventilatory cycle, varying by about 10 percent (tidal volume / functional residual capacity). In this sense the model is valid over a wide domain of space and time.

Regarding shape factors of neighboring alveoli and divergence of shape factor values with septal shift, one can argue rather convincingly that curvature dependent Laplace forces will cause an individual partially flattened alveolar gas bubble to round-up and to become more uniformly curved as much as possible, subject to local boundary conditions. Recall that actual gas/water interfaces are not preserved in the usual histologic preparations for light microscopy. Hence, we think of alveolar air spaces as more angulated than they really are. Shape factors would tend to bunch near the hemispherical value of $\varphi = 4$, as described previously. Nevertheless, modest linear changes in the shape factor in either direction with sepal shifts, described mathematically by the constant, k, in Equations (11b) through (13b), cause only modest changes in stability criteria, as shown, for example, in Figure 8 Overall, the perturbation analysis described here model is robust with respect to differences in initial alveolar size and shape.

In the absence of adequate surfactant activity, the neighboring bubble model of Figure 2 and Equation (13b) predicts local aggregation of gas volume into a few "giant" alveoli, with collapse of neighboring alveoli in the region. This pattern of pathology is exactly that observed in real-world cases of respiratory distress syndrome of the newborn[14, 42], which are characterized microscopically by multiple collapsed alveoli surrounding hyper-aerated alveoli, which are often lined with rims of amorphous protein deposits called hyaline membranes. Could the side by side bubble model also explain the other hallmark feature of respiratory distress syndrome of the newborn, namely the presence of hyaline membranes, which are composed of proteins and occasionally fibrin[42], lining the larger alveoli? Perhaps so.

Consider the shear stresses placed on a shared alveolar wall, containing a pulmonary capillary, as shown in Figure 9. Here the circumference of the capillary includes three endothelial cells, surrounding a plasma filled lumen containing one red blood cell, shown in dark shading. As one neighboring bubble enlarges and the other shrinks, one side of the capillary wall is stretched and

the other is compressed. This action may tend to pull apart cell-cell junctions between capillary endothelial cells on the stretched side selectively. Small gaps might well appear on the large bubble side of the capillary only. These gaps would be sufficiently wide to allow leakage of plasma proteins including fibrin monomers and other clotting factors, but not wide enough to allow escape of the much larger red blood cells. The leaked fibrin monomers would then tend to cross-link, forming a cell-free hyaline protein gel. In this way the local asymmetry of shear stress may explain the appearance of hyaline membranes within the larger, expanded gas bubbles, rather than within the smaller, collapsed ones.

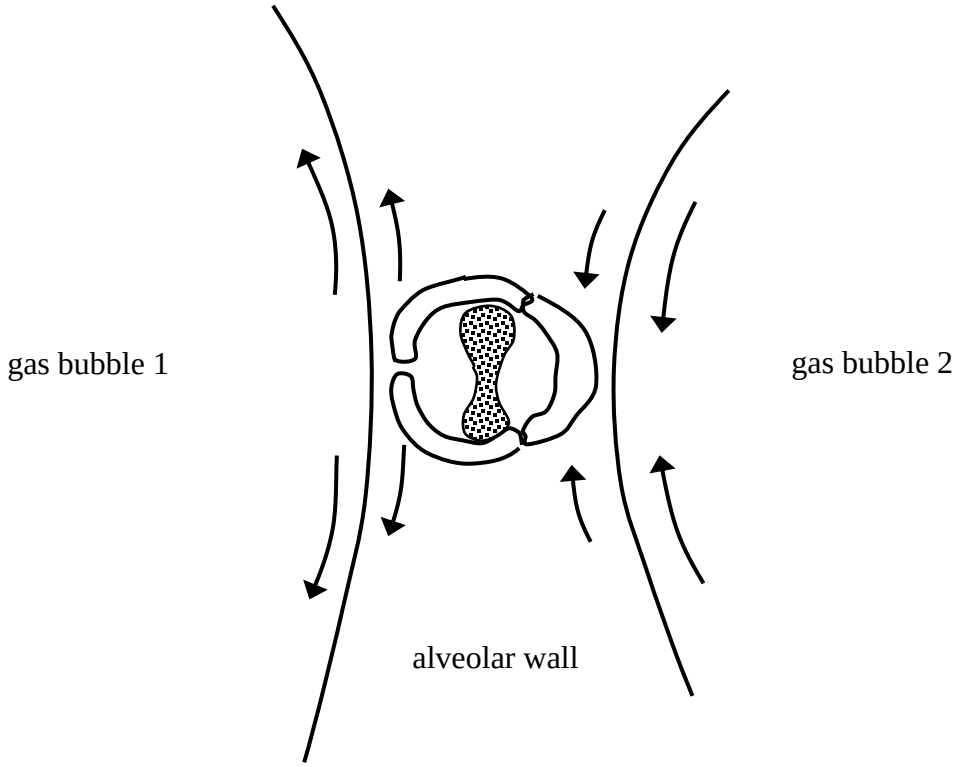

Figure 9. Scheme for explaining the formation of hyaline membranes. Opposing shear stresses tend to pull apart capillary endothelial cells on one side, allowing leakage of plasma proteins.

Note also that without adequate surfactant the adjacent bubble model of Figure 2 implies a cascading sequence of failure for clusters of multiple adjacent bubbles: A, B, C, D, …, within the same alveolar sac. If bubble A becomes transiently smaller, it will shrink and cause expansion of bubble B. Now, bubble B is larger than its other neighbor, C, which will tend to collapse into bubble B as well. If bubble B has more than the two neighbors, A and C, call them D, E, and F, originally of normal size, then those bubbles will also tend to collapse into B. This sequence predicts the creation of single large bubbles, surrounded by multiple smaller ones in the absence

of surfactant—exactly as is seen microscopically in cases of respiratory distress syndrome of the newborn[42].

The present theoretical treatment is, of course, highly simplified. Nevertheless, it does explain many facets of normal and abnormal physiology, including why protection from alveolar collapse provided by surfactant is normally quite robust, regardless of initial bubble diameter, intrathoracic pressure, regional variation in lung ventilation, or modest differences in surfactant composition or effectiveness; why without surfactant there are many tiny collapsed alveoli, and a few hyper-expanded, giant alveoli in a low power microscopic field; why hyaline membranes tend to appear mostly in larger alveoli; why there is not massive pulmonary edema in the lungs of premature babies with RDS of the newborn; why an inadequate dose of surfactant can lead to partial reversal without complete normalization of alveolar size disparity; why alveolar size discrepancies between lung lobes are allowed; and why bats and shrews, reported to have very small alveolar diameters compared to other mammals[44], can maintain these small alveolar diameters, even though smaller bubbles have higher transmural pressures.

5. CONCLUSIONS

The anatomically realistic adjacent bubble model described herein captures essential mechanisms underlying the action of pulmonary surfactant. It provides quantitative expressions that incorporate the physics of surface tension to explain how air-breathing land animals survive, despite air-water surface tension in the lungs. It also explains the pathophysiology and microscopic pathology of respiratory distress syndrome of the newborn, including the formation of hyaline membranes.

FUNDING SOURCES

Purdue University internal funds.

APPENDIX: estimation of constant, b, from experimental data

Consider two experimentally measured points 1 and 2 on the downward sloping linear range of the chart in Figure 3 and Equation (6). Point 1 represents a state of high surface tension and low surfactant concentration, and point 2 represents a state of lower surface tension and increased surfactant concentration. The slope between these points is

$$s = \frac{T_2 - T_1}{ln(c_2) - ln(c_1)} . \qquad (20)$$

In terms of the constants c_0 and c_{max}, representing the smallest and largest surfactant concentrations on the complete linear portion of the curve in Figure 3 from T_{max} to $(1 - \beta)T_{max}$, for maximum fractional reduction in surface tension, β, the slope of the middle linear portion is

$$s = \frac{(1-\beta)T_{max} - T_{max}}{ln(c_{max}) - ln(c_0)} . \quad (21)$$

Equating the two slopes, s < 0, in Equations (20) and (21), simplifying, and substituting ΔT for the absolute value of the surface tension difference between points 1 and 2,

$$\frac{\Delta T}{ln\left(\frac{c_2}{c_1}\right)} = \frac{\beta T_{max}}{ln\left(\frac{c_{max}}{c_0}\right)} . \quad (22)$$

The logarithmic function of constants, c_0 and c_{max}, can be determined from experimental data as

$$ln\left(\frac{c_{max}}{c_0}\right) = \frac{\beta T_{max}}{\Delta T} ln\left(\frac{c_2}{c_1}\right) . \quad (23)$$

Using Equation (9), substituting from Equation (23), and using the data for $\ln(c_2/c_1)$ in Table 1,

$$b = \beta \frac{2}{ln\left(\frac{c_{max}}{c_0}\right)} = \beta \frac{2}{\frac{\beta T_{max}}{\Delta T} ln\left(\frac{c_2}{c_1}\right)} = \frac{2\frac{\Delta T}{T_{max}}}{ln\left(\frac{c_2}{c_1}\right)} . \quad (24)$$

In this way one can estimate constant b from the measured relative surface tension reduction, $\Delta T/T_{max}$, and the surfactant concentration ratio, c_2/c_1, which produced $\Delta T/T_{max}$ experimentally.

REFERENCES

1. Schwartz R, Luby A, Scanlon J, Kellog R (1994). Effect of surfactant on morbidity, mortality, and resource use in newborn infants weighing 500 to 1500 g. New Engl J Med 330, 1476-1480.
2. Mandelbaum I, Giammona S (1964). Extracorporeal circulation, pulmonary compliance, and pulmonary surfactant. Thoracic and Cardiovascular Surgery 48, 881-889.
3. Ganong W (1991). Review of medical physiology. Appelton & Lang.
4. Hall S, Venkitaraman A, Whitsett J, Holm B, Notter R (1992). Importance of hydrophobic apoproteins as constituents of clinical exogenous surfactants. Am Rev Respir Dis 145, 24-30.
5. Zhang H, Wang Y, Fan Q, Zuo Y (2011). On the low surface tension of lung surfactant. Langmuir 27, 8351–8358.
6. Schurch S, Qanbar R, Bachofen H, Possmayer F (1995). The surface-associated surfactant reservoir in the alveolar lining. Biol Neonate 67 Suppl 1, 61-76.
7. Possmayer F, Nag K, Rodriguez K, Qanbar R, Schurch S (2001). Surface activity in vitro: Role of surfactant proteins. Comparative Biochemistry and Physiology Part A 129, 209-220.
8. Trillo J, Meijide F, Tato J, AJover, Soto V, deFrutos S, Galantini L (2014). Design of dialkyl surfactants from nitrilotriacetic acid as head group. RSC Advances 4, 6869-6877.
9. Sanderson RJ, Paul GW, Vatter AE, Filley GF (1976). Morphological and physical basis for lung surfactant action. Respir Physiol 27, 379-392.
10. Bachofen H, Hildebrandt J, Bachofen M (1970). Pressure-volume curves of air- and liquid-filled excised lungs-surface tension in situ. J Appl Physiol 29, 422-431.

11. Jonson B, Svantesson C (1999). Elastic pressure-volume curves: What information do they convey? Thorax 54, 82-87.
12. Liu JM, De Robertis E, Blomquist S, Dahm PL, Svantesson C, Jonson B (1999). Elastic pressure-volume curves of the respiratory system reveal a high tendency to lung collapse in young pigs. Intensive Care Med 25, 1140-1146.
13. Prange HD (2003). Laplace's law and the alveolus: A misconception of anatomy and a misapplication of physics. Adv Physiol Educ 27, 34-40.
14. Kumar V, Abbas A, Aster J (2014). Robbins & cotran pathologic basis of disease Elsevier.
15. Fung YC (1975). Does the surface tension make the lung inherently unstable? Circ Res 37, 497-502.
16. Hills B (1999). An alternative view of the role(s) of surfactant and the alveolar model. J Appl Physiol 87, 1567-1583.
17. Hills B (1981). Editorial: What is the true role of surfactant in the lung? Thorax 36, 1-4.
18. Farish SE, Garcia PS (2013). Capnography primer for oral and maxillofacial surgery: Review and technical considerations. J Anesth Clin Res 4, 295.
19. Fox SI (2007). Human physiology. McGraw-Hill
20. Wheeler D (2009). The respiratory tract in pediatric critical illness and injury. Springer-Verlag London Limited
21. Blanch PB (2009). Chapter 128 - anatomy of mechanical ventilation -- section xiii - respiratory disorders. Civetta, taylor, & kirby's: Critical care. Lippincott Williams & Wilkins.
22. Reifenrath R (1975). The significance of alveolar geometry and surface tension in the respiratory mechanics of the lung. Respir Physiol 24, 115-137.
23. Yu S, Harding P, Smith N, Possmayer F (1983). Bovine pulmonary surfactant: Chemical composition and physical properties. Lipids 18, 522-529.
24. Seeger W, Grube C, Gunther A, Shmidt R (1999). Surfactant inhibition by plasma proteins: Differential sensitivity of various surfactant preparations. Eur Respir J 6, 971-977.
25. Barrow R, Hills B (1979). Surface tension induced by dipalmitoyl lecithin in vitro under physiological conditions. J. Physiol 297, 217-227.
26. Bradley JM (2005). Determining the dispersive and polar contributions to the surface tension of water-based printing ink as a function of surfactant surface excess. Journal of Physics D Applied Physics 38, 2045.
27. Badawi AM, Mohamed MA, Mohamed MZ, Khowdairy MM (2007). Surface and antitumor activity of some novel metal-based cationic surfactants. J Cancer Res Ther 3, 198-206.
28. Otis D, Ingenito E, Kamm R, Johnson M (1994). Dynamic surface tension of surfactant ta: Experiments and theory. J Appl Physiol 77, 2681-2688.
29. Hallman M, Gluck L (1976). Phosphatidylglycerol in lung surfactant. Iii. Possible modifier of surfactant function. Journal of Lipid Research 17, 257-262.
30. Schurch S, Bachofen H, Goerke J, Possmayer F (1989). A captive bubble method reproduces the in situ behavior of lung surfactant monolayers. J Appl Physiol (1985) 67, 2389-2396.
31. Andreassen S, Steimle KL, Mogensen ML, Bernardino de la Serna J, Rees S, Karbing DS (2010). The effect of tissue elastic properties and surfactant on alveolar stability. J Appl Physiol (1985) 109, 1369-1377.
32. Smith JC, Stamenovic D (1986). Surface forces in lungs. I. Alveolar surface tension-lung volume relationships. J Appl Physiol (1985) 60, 1341-1350.
33. Schurch S, Goerke J, Clements JA (1978). Direct determination of volume- and time-dependence of alveolar surface tension in excised lungs. Proc Natl Acad Sci U S A 75, 3417-3421.

34. Kharge AB, Wu Y, Perlman CE (2014). Surface tension in situ in flooded alveolus unaltered by albumin. J Appl Physiol (1985) 117, 440-451.
35. West J (1979). Respiratory physiology: The essentials.
36. Clements J (1962). Surface tension in the lungs. Scientific American 207, 119-128.
37. Schurch S, Bachofen H, Possmayer F (2001). Surface activity in situ, in vivo, and in the captive bubble surfactometer. Comparative Biochemistry and Physiology Part A 129, 195-207.
38. Johansson J, Curstedt T, Robertson B. Compositions comprising pulmonary surfactants and a polymyxin having improved surface properties.
39. Klingele TG, Staub NC (1970). Alveolar shape changes with volume in isolated, air-filled lobes of cat lung. J Appl Physiol 28, 411-414.
40. Oldmixon EH, Hoppin FG, Jr. (1991). Alveolar septal folding and lung inflation history. J Appl Physiol (1985) 71, 2369-2379.
41. Perlman CE, Wu Y (2014). In situ determination of alveolar septal strain, stress and effective young's modulus: An experimental/computational approach. Am J Physiol Lung Cell Mol Physiol 307, L302-310.
42. Lauweryns JM (1970). "Hyaline membrane disease" in newborn infants. Macroscopic, radiographic, and light and electron microscopic studies. Hum Pathol 1, 175-204.
43. Clements J, Brown E, Johnson R (1958). Pulmonary surface tension and the mucus lining of the lungs: Some theoretical considerations. J Appl Physiol 12, 262-268.
44. Tenney S, Remmers J (1963). Comparative quantitative morphology of the mammalian lung: Diffusing area. Nature 197, 53-56.